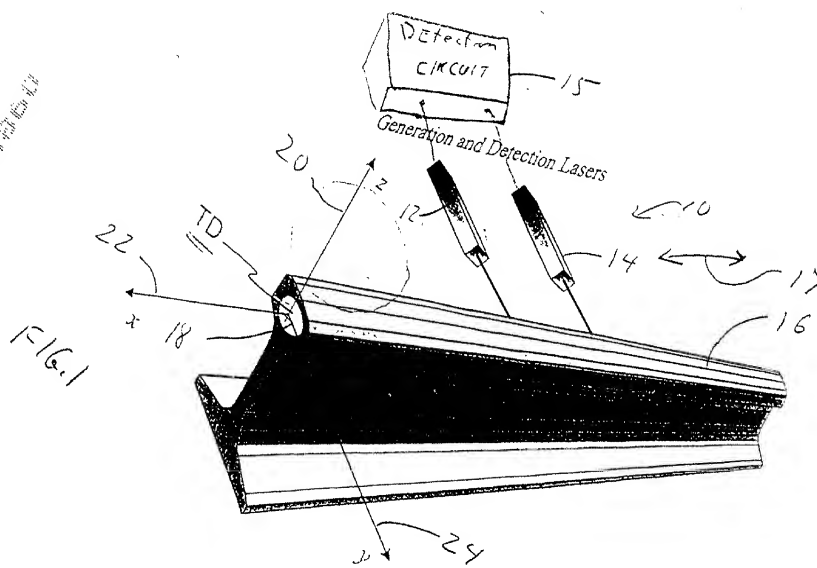


FIG. 1



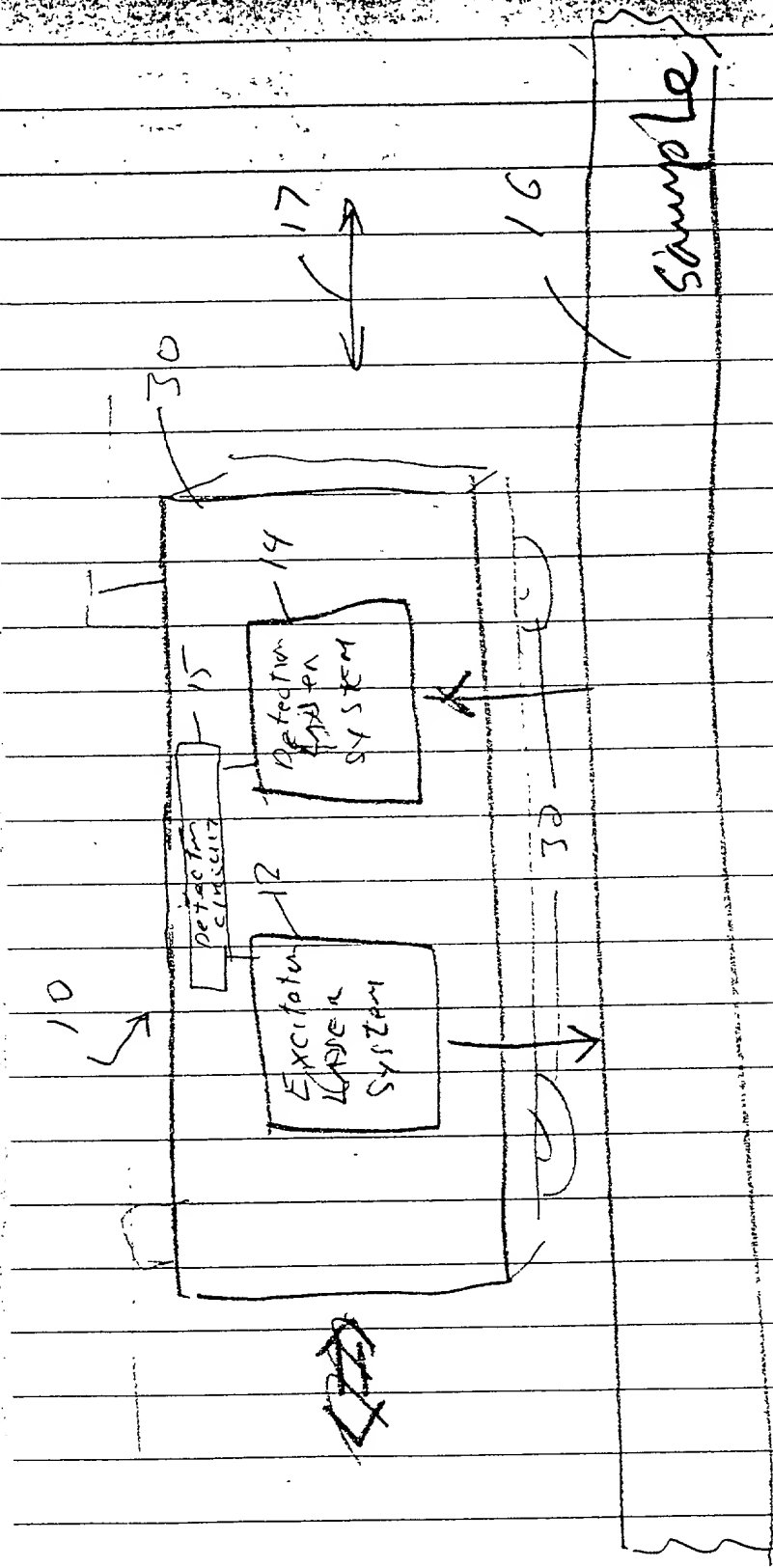


FIG. 2

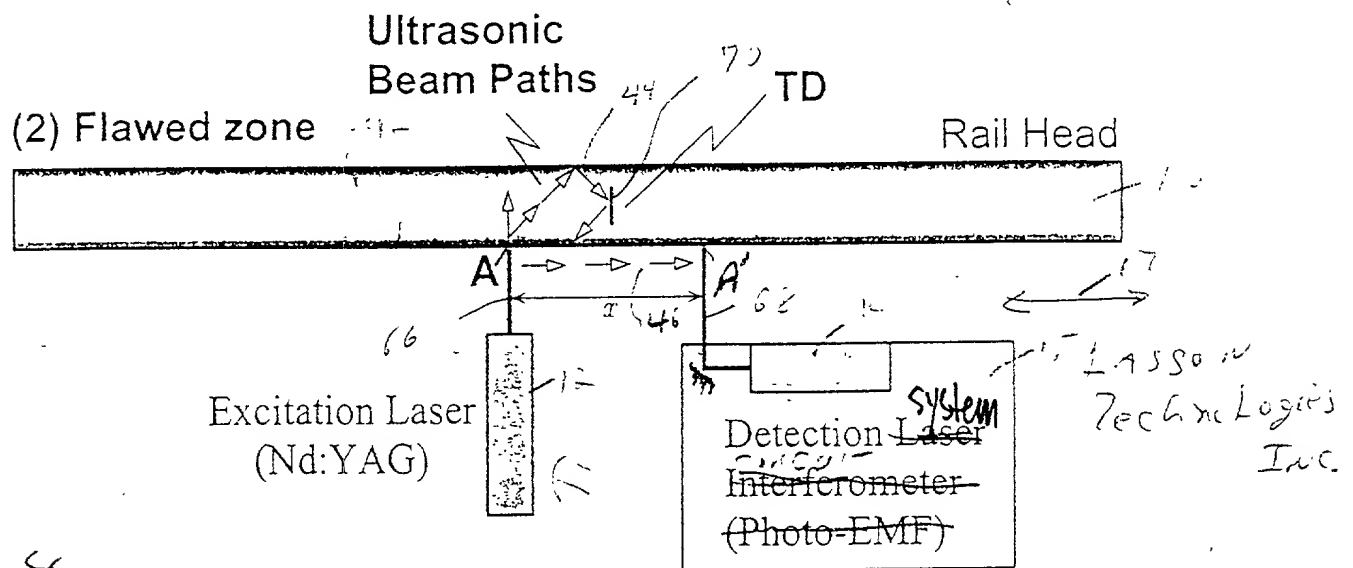
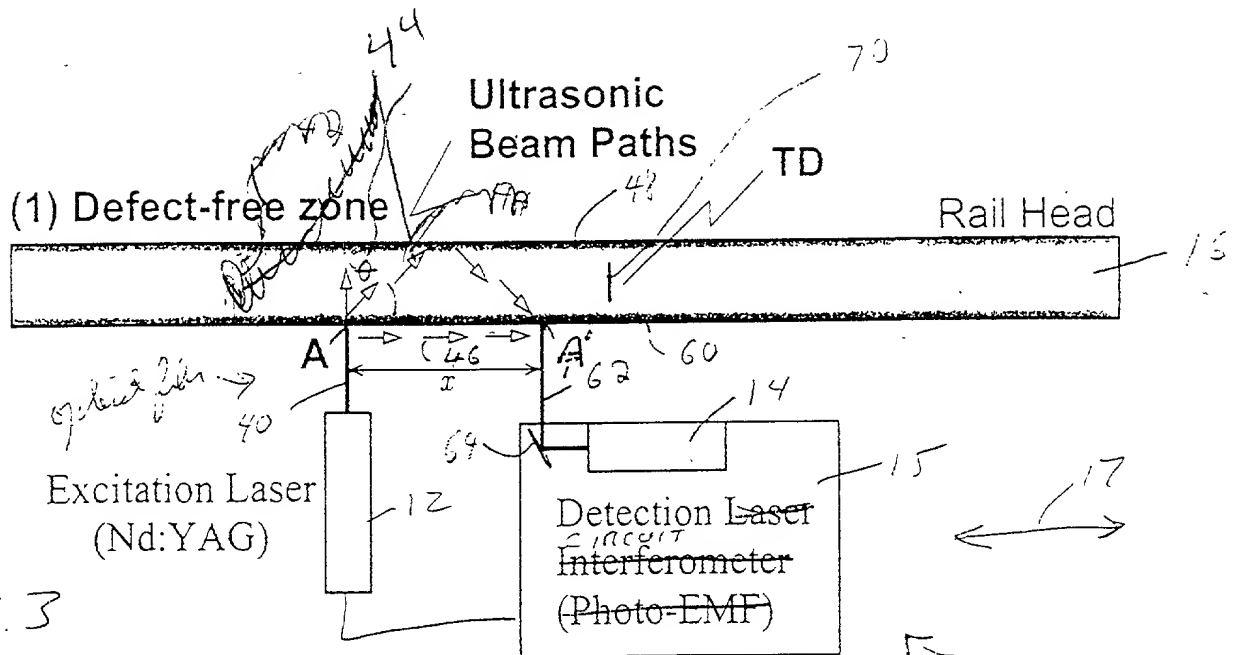
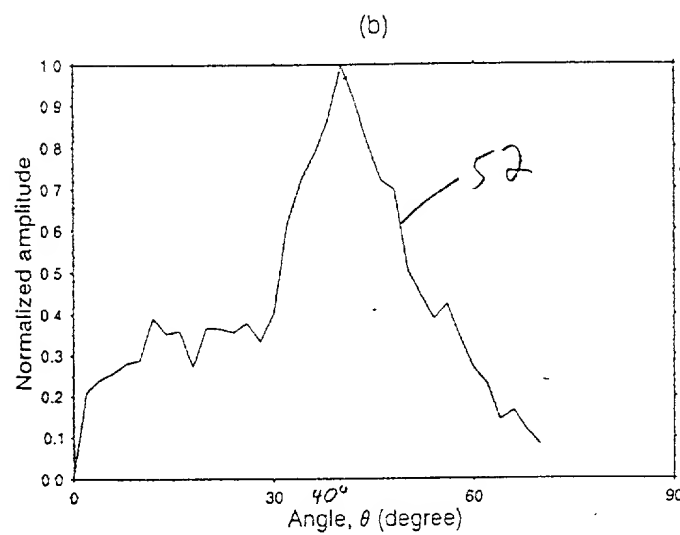
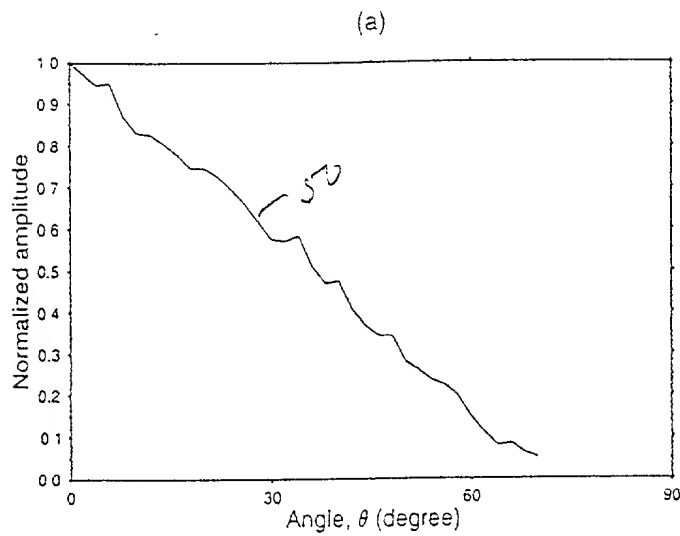


Figure 2: Proposed photoacoustic rail flaw detection scheme and the experimental setup used for conducting the proof-of-concept tests. Both excitation and detection lasers illuminate the same side of a rail sample containing a transverse defect.



RECEIVED
SEP 08 2000
TECHNOLOGY LICENSING OFFICE

Figure 4: The measured out-of-plane displacements as a function of propagating angle θ for the aluminum specimen: (a) longitudinal out-of-plane displacements (U_y^L); (b) shear out-of-plane displacements (U_y^T).

T05070-578666

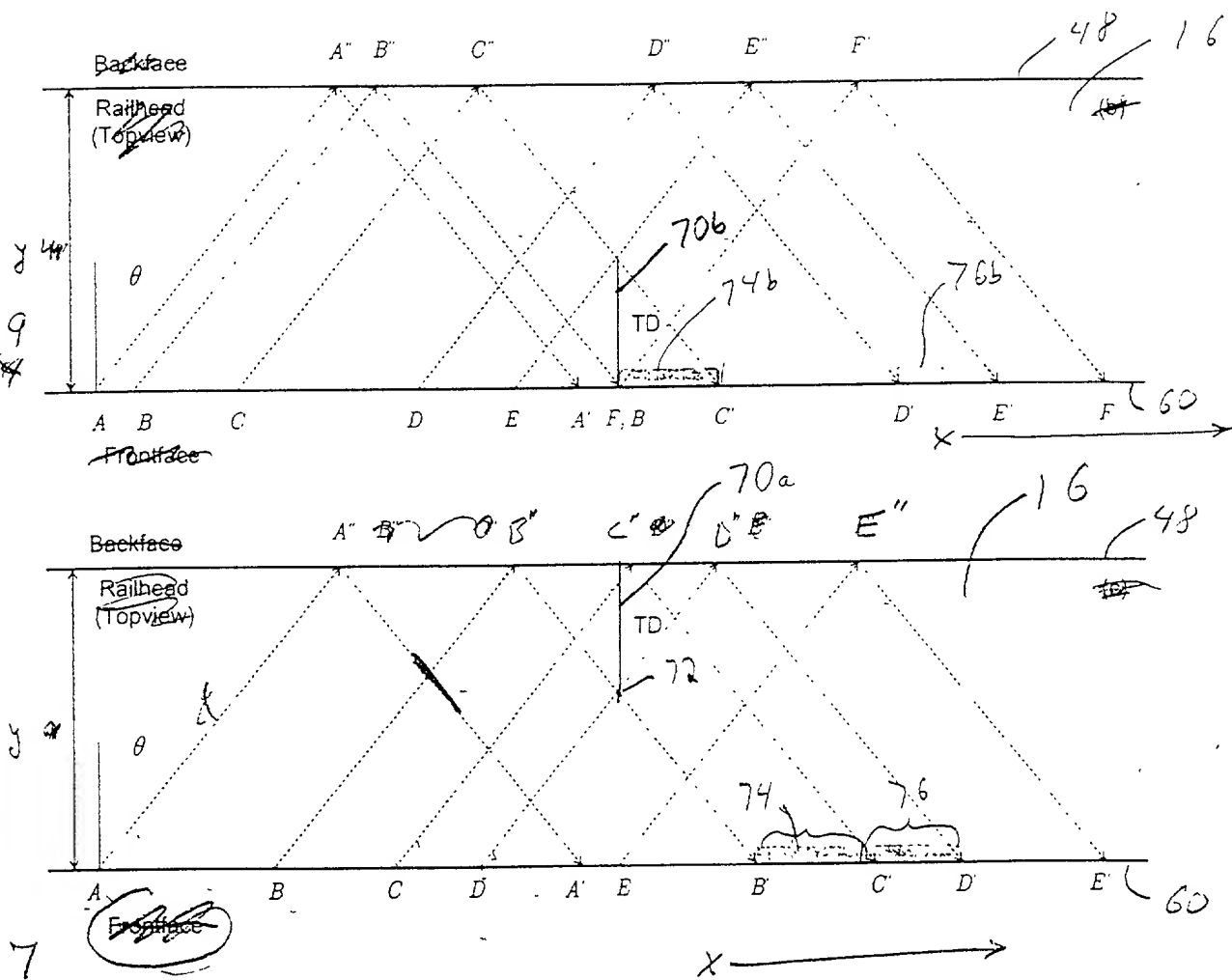


Figure 4: Three different rail railheads containing a transverse defect in each sample at different locations. The ultrasonic ray paths at various scanning positions are denoted by the dashed arrows.

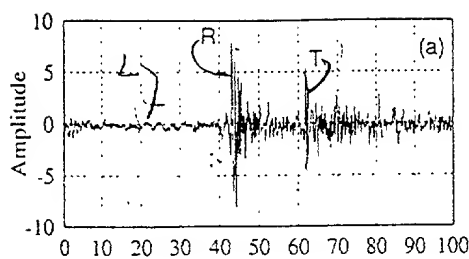


FIG. 8A

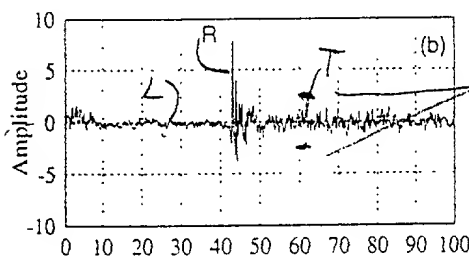


FIG. 8B

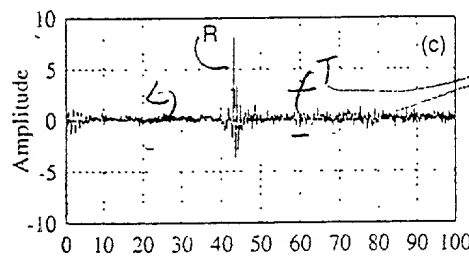


FIG. 8C

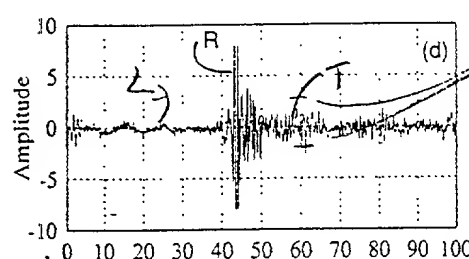


FIG. 8D

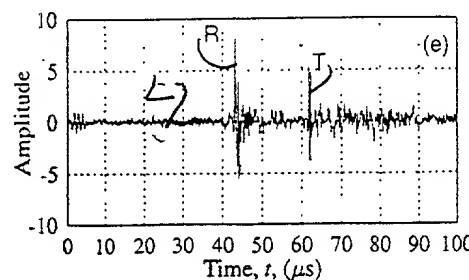
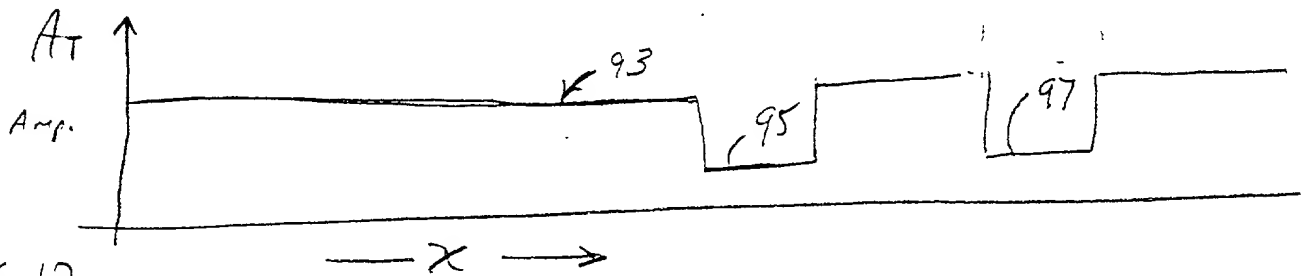
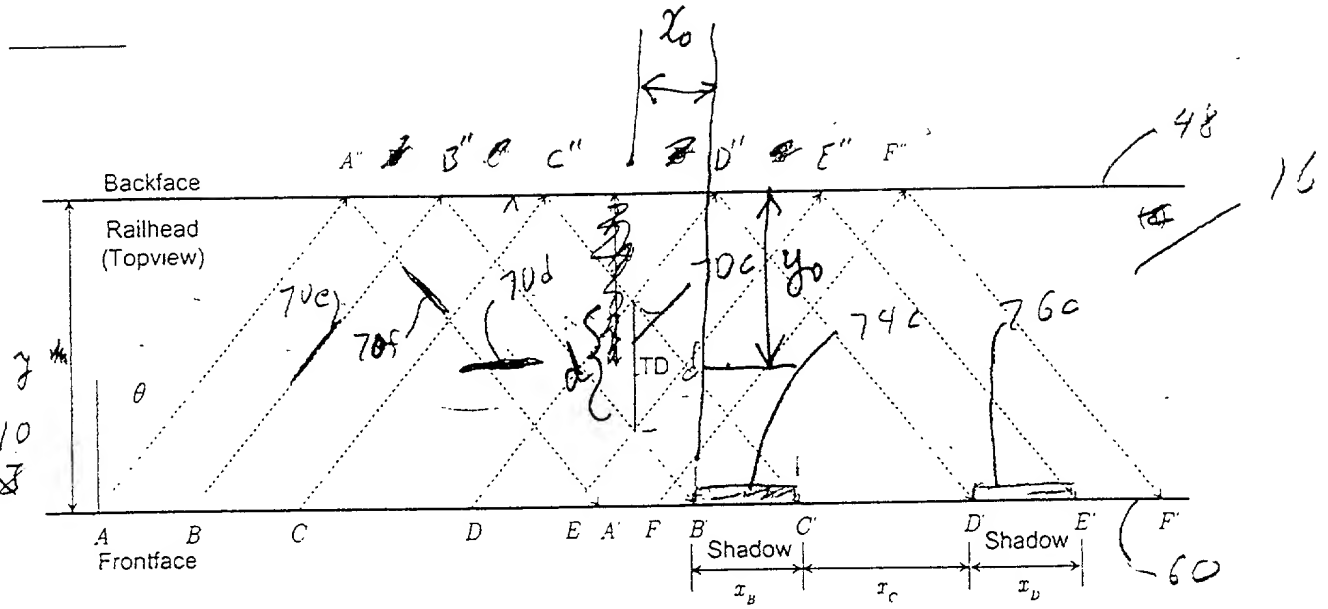


FIG. 8E

105040" 57886860

AT
Amp.
F16.12



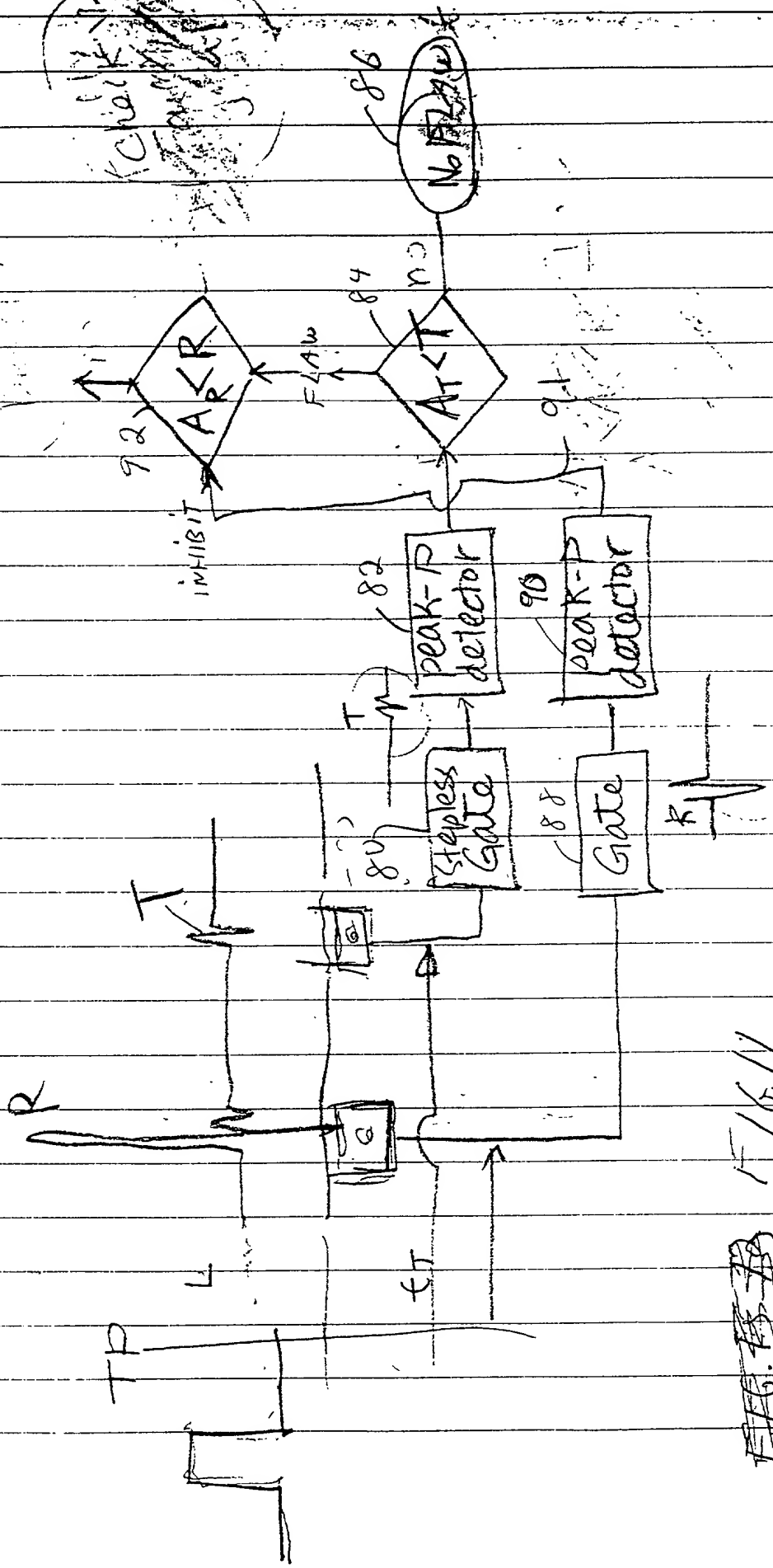


FIG. 13 1/6/11

Diagram for flaw detection

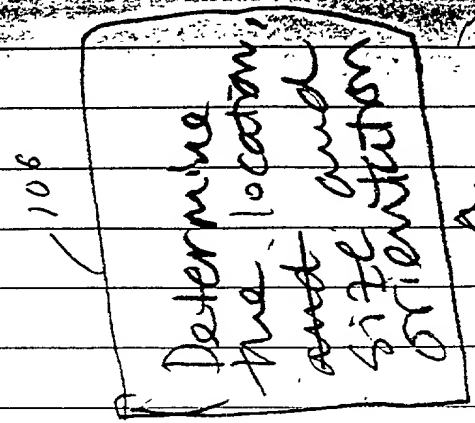
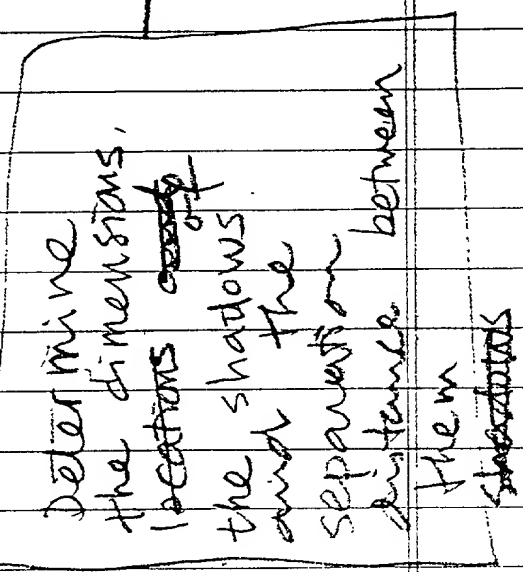
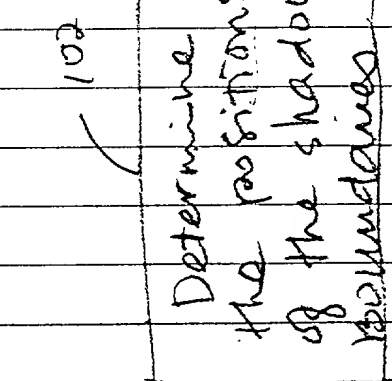
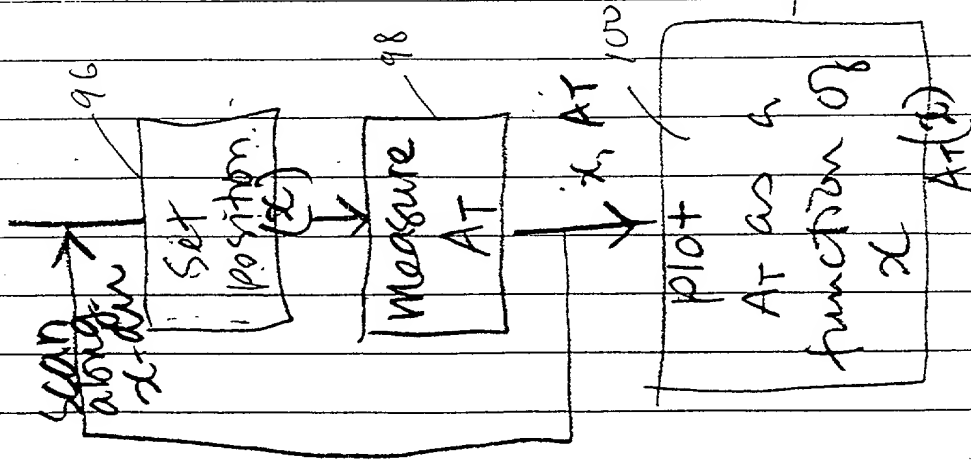
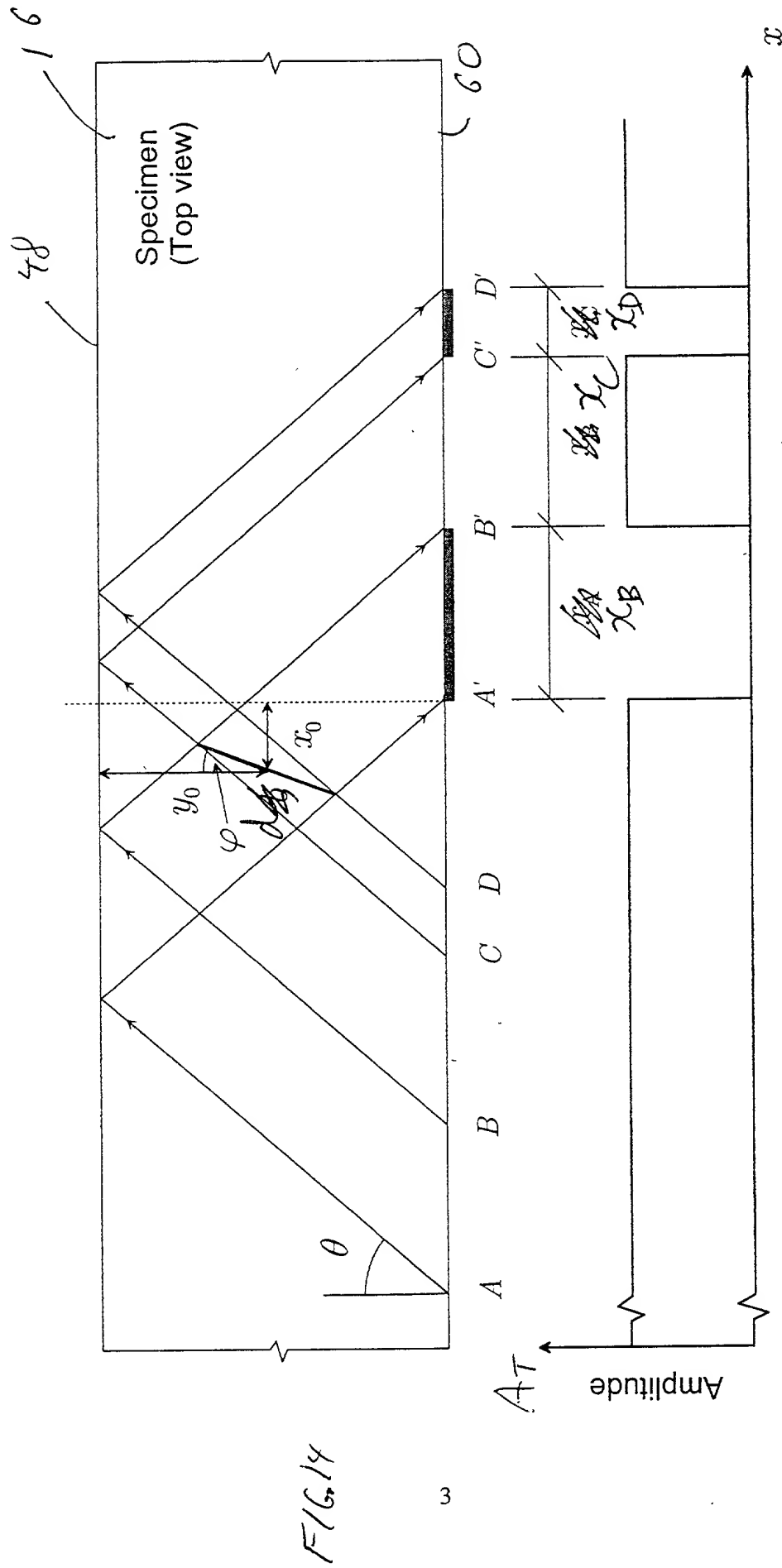


FIG. 13



51917

6791